Boundary-Layer Meteorology (2006) 121: 89–110
DOI 10.1007/s10546-005-9022-8

SCINTILLOMETER-BASED TURBULENT FLUXES OF SENSIBLE AND LATENT HEAT OVER A HETEROGENEOUS LAND SURFACE – A CONTRIBUTION TO LITFASS-2003

W. M. L. MEIJNINGER[1,*], F. BEYRICH[2], A. LÜDI[3], W. KOHSIEK[4] and H. A. R. DE BRUIN[1]

[1]*Meteorology and Air Quality Group, Wageningen University and Research Centre, Duivendaal 2, 6701 AP Wageningen, The Netherlands;* [2]*Meteorological Observatory Lindenberg, German Meteorological Service (DWD), Am Observatorium 12, 15848 Tauche – OT Lindenberg, Germany;* [3]*Institute of Applied Physics, University of Bern, Sidlerstr. 5, 3012 Bern, Switzerland;* [4]*Royal Netherlands Meteorological Institute (KNMI), P.O. Box 201, 3730 AE De Bilt, The Netherlands*

(Received in final form 28 July 2005 / Published online: 5 October 2005)

Abstract. The performance of a combined large aperture scintillometer (LAS) and a millimetre wave scintillometer (MWS) for estimating surface fluxes of sensible and latent heat over natural landscape is investigated, using data gathered during LITFASS-2003. For this purpose the LAS–MWS system was installed in a moderate heterogeneous landscape over a path length of 4.7 km with an effective beam height of 43 m. The derived surface fluxes have been compared with aggregated eddy-covariance (EC) measurements. The fluxes of sensible and latent heat from the LAS–MWS combination, as well as sensible heat fluxes of the single LAS, agreed fairly well with the EC-based fluxes, considering the uncertainties of the similarity stability functions and observed energy imbalance.

Keywords: Area-averaged surface fluxes, Evaporation, Heterogeneous area, Large aperture scintillometer, LITFASS-2003, Millimetre wave scintillometer, Scintillometer.

1. Introduction

Recent scintillometer studies have shown that the scintillation method is an interesting alternative for traditional point-measurements (e.g. the eddy-covariance (EC) method) of eddy heat fluxes, especially when one is concerned about the representativeness of *in situ* tower-based flux measurements over natural (and thus heterogeneous) landscapes (Lagouarde et al., 1996, 2002; Chehbouni et al., 2000; Beyrich et al., 2002a; Meijninger et al., 2002a,b). In most of these studies large aperture scintillometers (LAS) were used. This type of instrument works at a near-infrared wavelength

* E-mail: wouter.meijninger@wur.nl

($\lambda \sim 1$ μm) and is ideal for estimating the turbulent flux of sensible heat (H) over path lengths of several kilometres. The user friendliness and relative low manufacturing costs make it a popular instrument.

For latent heat flux ($L_v E$) measurements (where L_v is the latent heat of vaporisation), scintillometers that operate at radio to millimetre wavelengths are most suited. Until now the expensive technology, the complexity (e.g. temperature controlled units), absorption effects and required licences are the main reasons why such scintillometers have not been used as often as the near-infrared laser and large aperture scintillometers (Hill, 1997). Kohsiek and Herben (1983) were one of the first who succeeded in determining the surface latent heat flux using a single radio wave scintillometer (30 GHz). Hill et al. (1988) discuss the results of a millimetre wave scintillometer (173 GHz) and a near-infrared scintillometer (LAS) for estimating both the sensible and latent heat fluxes. It is known that the measurements of a single channel receiver can be distorted by low-frequency humidity fluctuations that have a spatial scale in the order of the scintillometer path length. Sarma and Hill (1996) describe a millimetre wave scintillometer (94 GHz) with a dual-channel receiver. By taking the variance of the difference of measured intensity fluctuations between the two receivers, instead of the variance of intensity fluctuations of one receiver, unwanted absorption effects are removed. Otto et al. (1996) discuss the results of this dual-channel receiver scintillometer by comparing the C_n^2 measurements with other scintillometers and *in situ* based C_n^2 data. Recent published studies are Green et al. (2000, 2001) and Meijninger et al. (2002b), who both used a (single receiver) radio wave scintillometer at 27 GHz in combination with a LAS, and made flux comparisons using EC observations. Meijninger et al. (2002b) systematically investigated the scintillometer combination over a moderate heterogeneous landscape. Formally, Monin-Obukhov Similarity Theory (MOST), which is used to derive the surface fluxes from the measurements, restricts the scintillation method to homogeneous areas. Meijninger et al. (2002a, b) found good agreement between the scintillometer fluxes and the aggregated fluxes based on several EC stations.

The combination of a near-infrared scintillometer and a millimetre wave scintillometer is also known as the two-wavelength method (Andreas, 1989, 1990, 1991). As noted by Andreas (1990), there are several shortcomings to this method; one of these is the remaining unknown structure parameter of the covariant term between temperature and humidity (C_{TQ}). This can be overcome by assuming a perfect correlation between temperature and humidity (Kohsiek and Herben, 1983; Hill et al., 1988; Hill, 1997). Due to this assumption the magnitude of H and $L_v E$ can be determined but not the sign (Andreas, 1990), implying that additional meteorological information is required to determine the sign of the fluxes. Several authors have proposed the use of three wavelengths (Kohsiek and Herben, 1983;

Hill et al., 1988; Andreas, 1990). However, technical, theoretical and financial aspects make this option less attractive (Kohsiek, 1982a; Hill, 1997). Recently, Lüdi et al. (2005) have shown that the bichromatic correlation of an optical and millimetre wave signal can be used to extract C_{TQ} (and r_{TQ}) directly, and found good agreement between the scintillometer and EC measurements. Their technique further reduces the dependency of the scintillation method on additional and mostly *in situ* data.

The main objective of our study is to investigate whether the two-wavelength method, using a LAS, a millimetre wave (94 GHz) scintillometer (further denoted as MWS) and *in situ* r_{TQ} data, can provide reliable area-averaged surface fluxes of sensible heat and in particular, the latent heat over a heterogeneous area. In addition, we also evaluate the sensible heat fluxes that can be derived from the single LAS. This study is part of the LITFASS-2003 experiment (Beyrich and Mengelkamp, 2006) and is also a continuation of LAS research (Beyrich et al., 2002a) that started in 1998 as part of LITFASS-98 (Beyrich et al., 2002b). Furthermore, this study is a continuation of the work of Lüdi et al. (2005) who focussed on the bichromatic correlation coefficient for deducing C_{TQ}. Here we will focus only on the scintillometer data, in particular the fluxes, collected during the LITFASS-2003 measurement campaign (21 May to 17 June 2003).

2. Theory: Two-Wavelength Method

The relation between the propagation statistics of the electromagnetic radiation (σ_χ^2, the variance of the natural logarithm of amplitude fluctuations) and the path-averaged structure parameter of the refractive index of air (C_n^2) for the LAS is as follows (Wang et al., 1978),

$$C_{n,\mathrm{LAS}}^2 = 4.48\sigma_\chi^2 D^{\frac{7}{3}} L^{-3}, \tag{1}$$

where D is the aperture diameter and L the path length. Ochs and Wilson (1993) found that this expression is valid (i.e. saturation free region) as long as

$$C_{n,\mathrm{LAS}}^2 < 0.193 L^{\frac{-8}{3}} \lambda^{\frac{2}{6}} D^{\frac{5}{3}}. \tag{2}$$

The relation between σ_χ^2 and C_n^2 for the MWS is as follows (Wang et al., 1978)

$$C_{n,\mathrm{MWS}}^2 = 8.06\sigma_\chi^2 k^{-\frac{7}{6}} L^{-\frac{11}{6}}, \tag{3}$$

where $k = 2\pi/\lambda$ is the optical wavenumber. This expression is valid for $\sigma_\chi^2 <$ 0.3 (Clifford et al., 1974; Wang et al., 1978).

The structure parameter of the refractive index of air for both the LAS and the MWS is related to turbulent temperature and humidity fluctuations as follows (Hill et al., 1980)

$$C_n^2(\lambda) = \frac{A_T^2(\lambda)}{\overline{T}^2} C_T^2 + \frac{2A_T(\lambda)A_Q(\lambda)}{\overline{TQ}} C_{TQ} + \frac{A_Q^2(\lambda)}{\overline{Q}^2} C_Q^2. \tag{4}$$

The variables A_T and A_Q are dependent on the wavelength of the electromagnetic radiation (λ), T is the absolute temperature and Q the absolute humidity (or water vapour density expressed in kg m^{-3}); expressions for A_T and A_Q for both the LAS and the MWS are given by Andreas (1988, 1990). In order to solve C_T^2, C_Q^2 and C_{TQ} from $C_{n,\mathrm{LAS}}^2$ and $C_{n,\mathrm{MWS}}^2$ (2 $\times$ Equation (4) with three unknowns), we define C_{TQ} as follows (Kohsiek, 1982b; Hill, 1997; Moene, 2003)

$$C_{TQ} = r_{TQ}\sqrt{C_T^2 C_Q^2}. \tag{5}$$

Instead of assuming a perfect correlation between temperature and humidity ($|r_{TQ}| = 1$, as required by MOST), which would result in two solutions for C_T^2 and C_Q^2 (and thus H and L_vE), we will use r_{TQ} data collected by a nearby EC system. As noted by Lüdi et al. (2005) measured r_{TQ} data (from either EC observations or the application of the bichromatic technique) will lead to better estimates of C_T^2, C_Q^2, and better fluxes, than those derived assuming $|r_{TQ}| = 1$.

By applying MOST we are able to derive H and L_vE from C_T^2 and C_Q^2 (Wyngaard et al., 1971)

$$\frac{C_T^2(z-d)^{\frac{2}{3}}}{T_*^2} = \frac{C_Q^2(z-d)^{\frac{2}{3}}}{Q_*^2} = f\left(\frac{z-d}{L_{Ob}}\right), \tag{6}$$

where f is a universal function of $\frac{(z-d)}{L_{Ob}}$, z is the effective height of the scintillometer beam, d is the zero-displacement height, with the Obukhov length $L_{Ob} = \frac{u_*^2 T}{g\kappa T_*}$ (with the von Kármán constant κ and the gravitational acceleration g), the temperature scale $T_* = \frac{-H}{\rho c_p u_*}$ (with the density of air ρ and the specific heat of air at constant pressure c_p), the humidity scale $Q_* = \frac{-E}{u_*}$ and the friction velocity u_*. The fluxes H and L_vE are solved iteratively, where the friction velocity is derived from wind speed data measured at one level and the effective surface roughness (z_0), using standard flux–profile relationships (see e.g. Panofsky and Dutton, 1984). The procedure is similar to the derivation of H from a single LAS (see e.g. De Bruin et al., 1995). Detailed information of the measurement heights and the roughness lengths are given in Section 3.

Several expressions can be found in the literature for f (Wyngaard et al., 1971; Andreas, 1988; De Bruin et al., 1993). Here, we will apply two rather extreme expressions, namely

$$f\left(\frac{z-d}{L_{Ob}}\right)=4.9\left(1-6.1\frac{z-d}{L_{Ob}}\right)^{\frac{-2}{3}} \tag{7}$$

from Andreas (1988),

$$f\left(\frac{z-d}{L_{Ob}}\right)=4.9\left(1-9\frac{z-d}{L_{Ob}}\right)^{\frac{-2}{3}} \tag{8}$$

from De Bruin et al. (1993), to determine the uncertainty of the mean fluxes H and L_vE (the mean flux F is defined as $\overline{F}=\frac{F_{\text{Andreas}}+F_{\text{DeBruin}}}{2}$ and the uncertainty as $\partial\overline{F}=\frac{|F_{\text{Andreas}}-F_{\text{DeBruin}}|}{2}$). We confine ourselves to unstable conditions only (i.e. $L_{Ob}<0$).

The surface flux of sensible heat can also be derived from the single LAS (i.e. without a MWS, see e.g. De Bruin et al., 1995). For the derivation of C_T^2 (and H) from $C_{n,\text{LAS}}^2$ we use a simplified expression for Equation (4) (Wesely, 1976). In this expression C_{TQ} and C_Q^2 are replaced by a 'correction-term' that contains the Bowen ratio ($Bo=H/L_vE$). Instead of taking a representative (constant) value for Bo we implemented the energy balance ($R_n=H+L_vE+G$, using net radiation (R_n) and soil heat flux (G) data) in the iteration procedure. In the case where R_n and G data are not available the first option gives similar results. In Section 4 we will study the fluxes from the LAS-MWS combination ($H_{\text{LAS-MWS}}$ and $L_vE_{\text{LAS-MWS}}$) as well as the sensible heat flux from the single LAS (H_{LAS}).

3. Experimental Site and Measurements

3.1. Experimental site and set-up

In Figure 1 the eastern part of the ($20\times20\,\text{km}^2$) LITFASS area is shown together with the LAS–MWS path. The western part of the LITFASS area (see Figure 2 of Beyrich and Mengelkamp, 2006) is covered mainly with forest (≈43% of total LITFASS area), while the eastern part (see Figure 1) mainly consists of agricultural fields and meadows (≈45% of total area). The remaining part is occupied by lakes (≈7%) and small built-up areas (≈5%). The farmland part of the LITFASS area, where the LAS–MWS is situated, consists of medium-size fields (typical size of 5–25 ha), separated by small patches of forest and hedges, where mostly cereals, rape and maize are grown. More detailed information can be found in Beyrich et al.

Figure 1. Eastern part of the LITFASS area ($11 \times 8\,km^2$) showing the source area of the LAS–MWS combination (white = open water; black = forest; dark grey = grass; medium grey = cereals; light grey = rape). The white line represents the path of the LAS–MWS, between the transmitter and receiver units, which are situated in Falkenberg (T) and Lindenberg (R), respectively.

(2002a) and Beyrich and Mengelkamp (2006). We estimated the effective roughness length for the area directly surrounding the scintillometers to be 0.2 m (procedure is based on the analysis of a topographical map (1:25000) according to Troen and Petersen (1989) who made a distinction between four different land surface classes (Foken and Göckede, personal communication, 2004)).

Figure 2 shows the cross-section of the LAS–MWS set-up between the 99-m meteorological tower in Falkenberg (transmitter site) and the 30-m tower at the observatory in Lindenberg (receiver site), which is situated on a small hill. The path length is 4.7 km and the effective height of the scintillometers is 43.3 m (±0.1 m depending on the atmospheric stability)

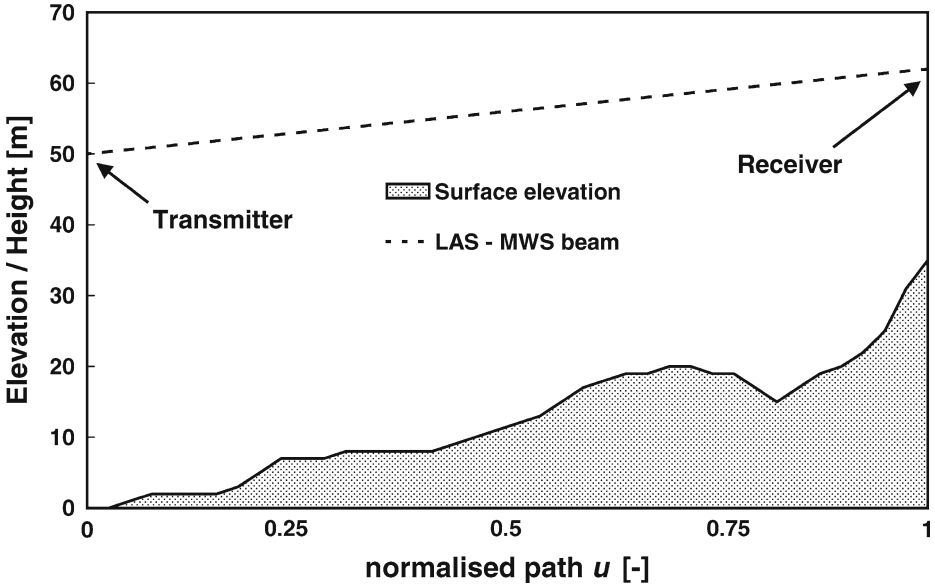

Figure 2. Cross-section of the scintillometer set-up between the 30-m tower at the Lindenberg observatory (north: receiver site) and the 99-m meteorological tower in Falkenberg (south: transmitter site). The base of the Falkenberg tower is taken as the zero reference.

following the procedure of Hartogensis et al. (2003), which incorporates the height dependency of C_T^2. The zero-plane displacement height (d) is considered to be zero, since no dense forest is present near the centre of the path of the scintillometers.

3.2. Measurements and data processing

The near-infrared LAS ($\lambda = 930\,\text{nm}$, $D = 0.15\,\text{m}$) was developed and built by the Meteorology and Air Quality Group of the Wageningen University; technical details are given in Meijninger et al. (2002a). The LAS has been operational at Lindenberg since May 1998 (Beyrich et al., 2002a) when LITFASS-98 commenced (Beyrich et al., 2002b). Ten-minute statistics of the output signals (band-pass filtered $C_{n,\text{LAS}}^2$ signal and signal strength) of the LAS (sample rate 1 Hz) are stored on a small built-in datalogger (BL1500, Z-World, Davis, CA, U.S.A).

The MWS was developed and built by the Institute of Applied Physics of the University of Bern (Switzerland), and operates at a wavelength of 3.2 mm (94 GHz) with an antenna diameter of 0.4 m. The raw output signal of the MWS was low-pass filtered at 20 Hz, sampled at 40 Hz and finally stored on disk for further processing. Post-processing involved spectral analysis of the signal that was band-pass filtered between 0.06 and 20 Hz using a 16.6-s moving average. Band-pass filtering was used

to remove low-frequency fluctuations that might be related to humidity absorption fluctuations, gain drift and changes in atmospheric opacity. As a check we calculated $C^2_{n,\mathrm{MWS}}$ using a 50-s moving average (i.e. 0.02 Hz), and found no notable change in $C^2_{n,\mathrm{MWS}}$. Also Lüdi et al. (2005) showed that the influence of absorption at 94 GHz is small.

10-minute $C^2_{n,\mathrm{MWS}}$ values were derived from the integrated 10-min power spectrum of log-amplitude fluctuations. A 10-min averaging period was chosen instead of 30-min in order to avoid non-stationary turbulent conditions. The spectral derivation of $C^2_{n,\mathrm{MWS}}$ was chosen in order to remove wind induced resonant frequencies of the 99-m tower (booms and guys), which were sometimes present in the spectra during strong wind conditions. An example of a 10-min spectrum of the MWS is depicted in Figure 3a, showing resonance peaks at 1.5 and 10 Hz. As a comparison we have plotted the corresponding theoretical spectrum of the MWS (Clifford, 1971). It is clearly seen that the measured spectrum reveals much more energy in the low frequency part of the spectrum (< 0.1 Hz). To explain this we have plotted also the measured and theoretical intensity spectrum of the LAS (Nieveen et al., 1998); the measured spectrum of the LAS shows the same 'increase' at low frequencies. Note that the peak at 50 Hz, which is insignificant, is related to the net power supply and not to tower vibrations. Based on the analysis of many LAS and MWS spectra we believe that the increase at low frequencies is related to slow tower movements (oscillations) induced by the wind (for $u_{40\mathrm{m}} > 6\,\mathrm{m\,s^{-1}}$). Unfortunately, we cannot confirm this hypothesis, as no tilt sensors (or accelerometers) were installed on the tower to measure vibrations. In order to be certain that excessive vibrations did not disturb our intercomparison study (Section 4) we have rejected MWS data for situations when the wind speed at 40 m was more than $6\,\mathrm{m\,s^{-1}}$. Figure 3b shows the spectra of the LAS and MWS for a 10-min period when the wind speed is less than $6\,\mathrm{m\,s^{-1}}$. It can be seen that for this case (and many others) the resonance peaks and slow tower oscillations are not present and the measured and theoretical spectra agree well.

Finally, the C_n^2 data from both the LAS and the MWS were averaged to 30-min values and checked for saturation, before being processed to fluxes; for $C^2_{n,\mathrm{LAS}}$ larger than $1.3 \times 10^{-14}\,\mathrm{m^{-2/3}}$ the data were rejected (according to the saturation criterion given in Equation (2)). The saturation criterion for the MWS ($C^2_{n,\mathrm{MWS}} < 6 \times 10^{-11}\,\mathrm{m^{-2/3}}$) was never reached. Additional observations (e.g. u, T and r_{TQ}) required for the derivation of the fluxes were taken from the 99-m tower from nearby levels (state variables at 40 m and r_{TQ} at 50 m). Note that the EC station that provided the r_{TQ} data has not been used in the flux intercomparison study (Section 4).

In total, 11 days of LAS–MWS data have been collected during LITFASS-2003 (19 May to 29 May); unfortunately, after 29 May the MWS broke down due to technical problems. Of these 11 days, 10 days only will be

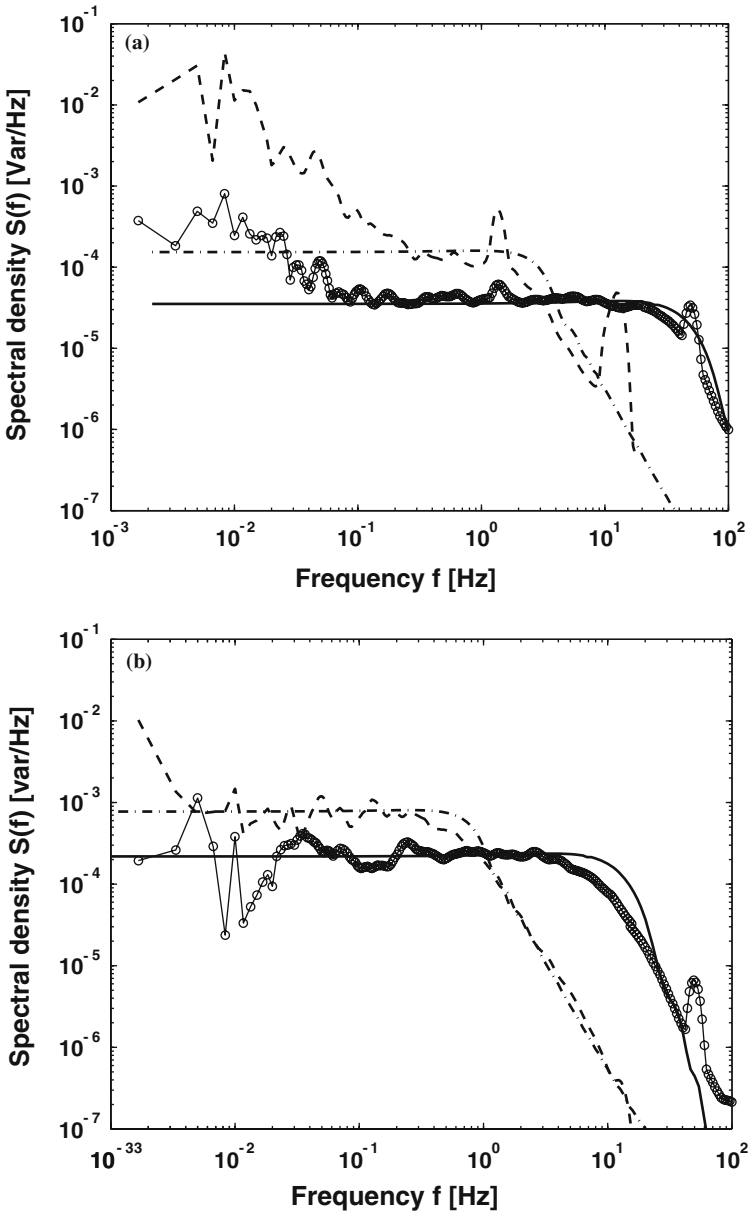

Figure 3. (a) Measured non-filtered 10-min intensity spectrum of the MWS (dashed), corresponding theoretical spectrum (dashed–dotted), measured intensity spectrum of the LAS (solid, circles) and corresponding theoretical spectrum (thick solid) for 20 May, 0820 to 0830 UTC ($u_{40} > 6\,\mathrm{m\,s^{-1}}$). (b) As Figure 3a except for 25 May, 1450 to 1500 UTC ($u_{40} < 6\,\mathrm{m\,s^{-1}}$).

presented here, since days with rain were rejected. In the morning and evening of 19 May about 5 mm of precipitation was recorded, followed by a dry period that was shortly interrupted on 23 May (1 mm) (Beyrich and Mengelkamp, 2006).

3.3. Surface heterogeneity – footprint analysis

Figure 1 shows that the horizontal scale of the forest and the farmland area (taken as a whole) on the LITFASS study region is on the order of 10 km (for further details the reader is referred to Figure 2 of Beyrich and Mengelkamp, 2006). This implies that, for this so-called type-B landscape, not only the surface layer, but also the atmospheric boundary layer, will be affected by these large-scale inhomogeneities (Shuttleworth, 1988; De Bruin, 1989). This has been supported by the Helipod flux-profile measurements of sensible heat flux profiles, which showed the individual surface characteristics of forest, open water and farmland are still recognizable up to heights of about 0.4 to 0.5 the convective boundary-layer height (corresponds to heights between 400 and 800 m) (see Bange et al., 2006).

One way to interpret measurements over heterogeneous areas is to use a footprint model, although one must keep in mind that these models can be inaccurate over complex areas. We have used in this study the analytical footprint model of Horst and Weil (1992, 1994) to estimate the source area (SA) of *in situ* measurements and the relative contribution of the various ground covers. The SA of a scintillometer can be estimated by combining the footprint model with the path weighting function of the scintillometer (Meijninger et al., 2002a, b). Finally, the relative contribution of each surface type to the measured flux can be estimated by combining the SA with a land-use map. The fractional covers per wind sector (45°) are shown in Figure 4, where it can be seen that farmland contributes up to 90% to the measured LAS–MWS fluxes. The error bars show the slight dependency on variations in atmospheric stability. The contribution of water was found to be less than 1%.

In this study we have made the distinction between forest (open water) and farmland (see Figure 4). In total 14 EC stations (mostly consisting of CSAT3 (Campbell Scientific) or USA-1 (METEK) sonic anemometers in combination with LI-7500 (Licor Inc.) or KH20 (Campbell Scientific) hygrometers) monitored the surface fluxes of the different land surface types. Some surface types were monitored by more than one EC station (Beyrich and Mengelkamp, 2006; Beyrich et al., 2006). Data processing (plus corrections), quality and footprint tests of the EC measurements were made by Mauder et al. (2006); Beyrich et al. (2006) provided the composite surface fluxes and corresponding uncertainties. The farmland, which gives the representative surface fluxes, is composed of rape, cereals, maize and grass, thereby accounting for their fractional cover within the LITFASS

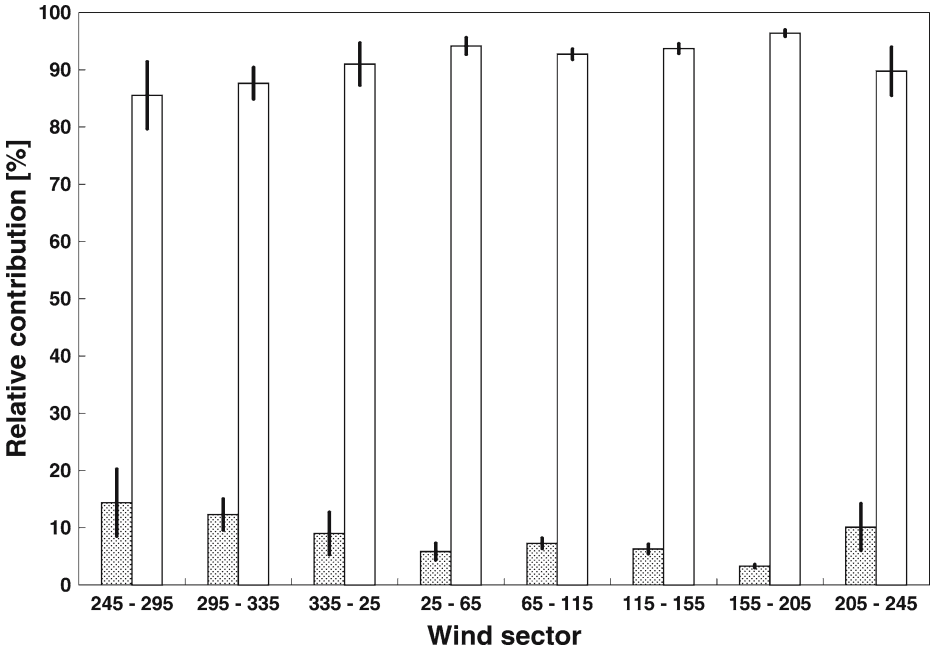

Figure 4. The relative contribution of forest and farmland for the eight wind sectors (45°). The total contribution per sector is 100%. The error bars represent the variation of contribution related to variations of atmospheric stability.

area ($20 \times 20\,km^2$). Although quite significant differences were found in the magnitude of the 'farmland' fluxes over the different crops (Beyrich and Mengelkamp, 2006; Beyrich et al., 2006), we will make no further distinction of farmland in this study. We expect that the 'signatures' of the different agricultural crops will have (partly) blended once transported to the scintillometer height, since the horizontal scale of most fields is relatively small.

4. Results

4.1. Fluxes of sensible and latent heat

In this section, we compare the sensible heat and latent heat fluxes from the LAS–MWS combination (10 days) as well as the sensible heat fluxes from the single LAS (30 days) against aggregated EC fluxes. In Figure 5 the sensible heat fluxes of the LAS are compared with the aggregated EC sensible heat fluxes; the error bars represent the uncertainties in the half-hour fluxes. The uncertainty in the LAS fluxes is the geometric mean of all individual uncertainties in the flux caused by uncertainties in each input

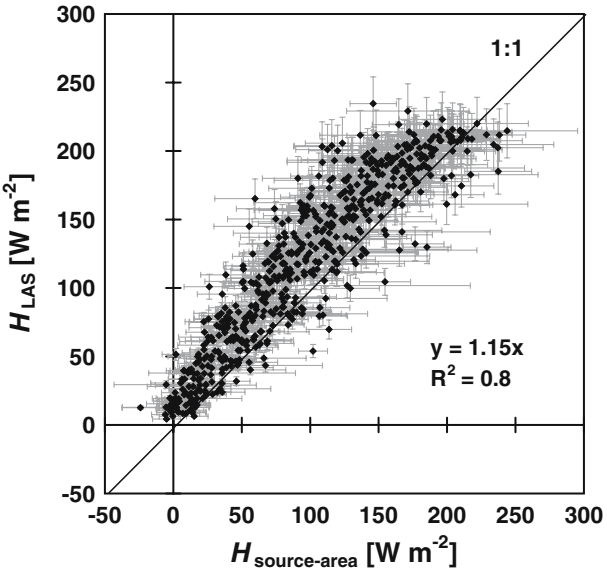

Figure 5. Scatter plot of the sensible heat fluxes of the single LAS versus the aggregated EC fluxes for a period of 30 days. Each point is a 30-min measurement. The error bars represent the uncertainty of the fluxes.

variable (i.e. z_o (50%), z_{LAS}, z_{MWS} and z_{u} (all 1%), L (2%), u and T (both 5%), r_{TQ} (25%), MOST stability functions (see Section 2), and R_n, G_s (the latter two are only used for the single LAS)). The values of these uncertainties are based on systematic errors as well as on the spatial variation of these variables along the path of the scintillometers. A regression analysis of Figure 5 yields: $H_{\mathrm{LAS}} = 1.15 H_{\mathrm{source-area}}$ and $R^2 = 0.8$. Although the error bars of many points straddle the 1:1 line it can be seen that the LAS gives systematically higher fluxes. This effect is also noticeable in Figure 6 where the sensible heat fluxes from the LAS–MWS combination are compared with the aggregated EC fluxes. A regression analysis yields: $H_{\mathrm{LAS-MWS}} = 1.07 H_{\mathrm{source-area}}$ and $R^2 = 0.83$. Although the LAS data have been checked for saturation effects (see Section 3.2) both figures imply that the LAS is experiencing saturation problems at high fluxes ($H_{\mathrm{LAS}} > 200\,\mathrm{W\,m^{-2}}$) (see Section 5).

In Figure 7 the latent heat fluxes of the LAS–MWS combination are plotted against the aggregated EC-based latent heat fluxes; the overall plot is similar to that for the sensible heat flux results. A regression analysis yields: $L_v E_{\mathrm{LAS-MWS}} = 1.26 L_v E_{\mathrm{source-area}}$ and $R^2 = 0.87$. For some reason the LAS–MWS fluxes of latent heat are about 26% higher than the EC fluxes. Meijninger et al. (2002b) found a difference of only 8%, based on a LAS–MWS combination using an identical LAS but with a different MWS (27 GHz).

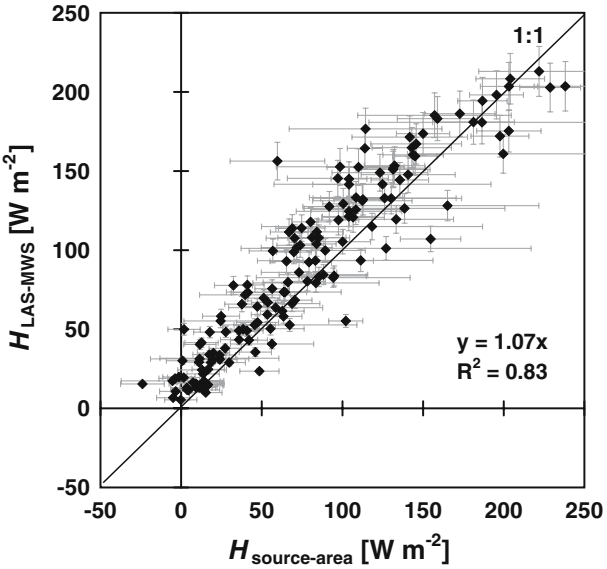

Figure 6. Scatter plot of the sensible heat fluxes of the LAS–MWS versus the aggregated EC fluxes for a period of approximately 10 days. Each point is a 30-min measurement. The error bars represent the uncertainty of the fluxes.

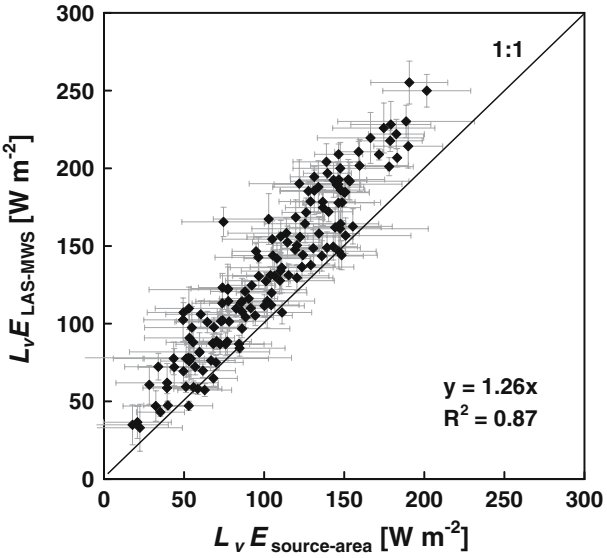

Figure 7. Scatter plot of the latent heat fluxes of the LAS–MWS versus the aggregated EC fluxes. Each point is a 30-min measurement. The error bars represent the uncertainty of the fluxes.

4.2. Surface energy balance closure

In Section 4.1 we found that the sensible heat fluxes from the LAS–MWS combination did agree reasonably well with the aggregated EC fluxes. For the latent heat fluxes, however, a significant deviation was found (26%). One plausible explanation for these results is the energy-balance closure of the LAS–MWS combination and the aggregated EC stations. In Figures 8 and 9 the energy balance closures of the LAS–MWS combination and the aggregated EC systems are shown, respectively. In these figures the measured sum of the turbulent fluxes H and L_vE is plotted against the aggregated available energy, i.e. the net radiation minus the storage in the soil. Mauder et al. (2006) discuss in detail the *in situ* radiation and soil heat flux measurements at all measurement sites. Liebethal et al. (submitted) performed a sensitivity study between the applied methods, namely the heat flux plates and gradient approach in combination with calorimetry, for estimating the soil heat flux at the surface. Here, we have aggregated the *in situ* net radiation and soil heat flux data in the same way as the fluxes H and L_vE. A regression analysis of Figure 8 yields: $(H+L_vE)_{\mathrm{LAS-MWS}} = 0.86(R_n-G)_{\mathrm{source-area}}$ and $R^2=0.85$. Meijninger et al. (2002b) found a closure of 95%. A regression analysis of Figure 9 yields: $(H+L_vE)_{\mathrm{source-area}} = 0.72(R_n-G)_{\mathrm{source-area}}$ and $R^2=0.93$. In Figure 9 it is obvious that the

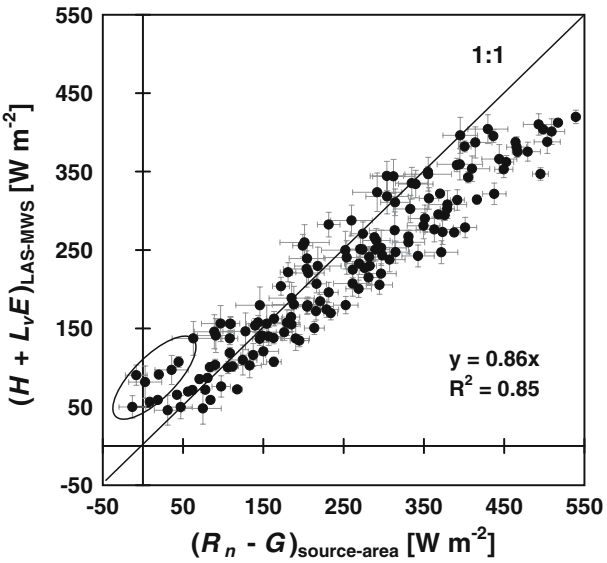

Figure 8. Scatter plot of $(H+L_vE)$ from the LAS–MWS versus the aggregated net radiation minus soil heat flux (R_n-G). Each point is a 30-min measurement. The vertical error bars represent the uncertainty of the fluxes. The horizontal error bars represent the variation of available energy using an uncertainty for R_n of 5% and for G of 15% (Mauder et al., 2006).

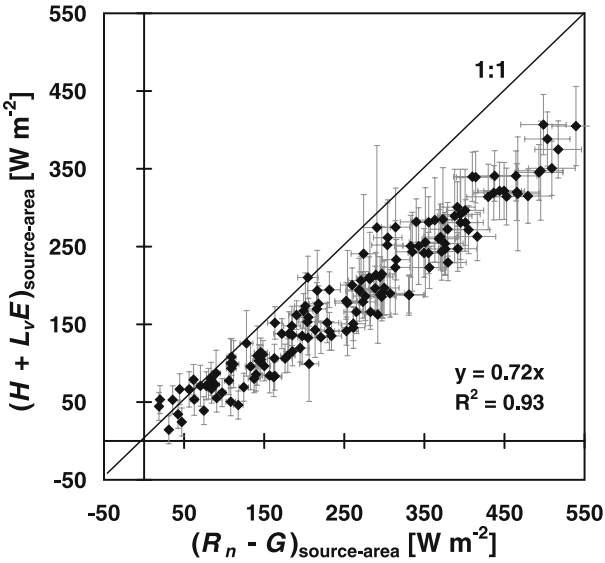

Figure 9. As Figure 8 except for the aggregated EC fluxes $(H + L_v E)_{\text{source-area}}$.

aggregated EC stations show an energy imbalance of almost 30%, and is present over the whole range of $(H + L_v E)$. Mauder et al. (2006) found approximately the same imbalance for the individual EC stations.

In Figure 8 the LAS–MWS combination shows an energy deficit at high fluxes while at low fluxes ($<150\,\mathrm{W\,m^{-2}}$) a slight surplus of energy is found (see encircled data points in Figure 8). As mentioned before, the energy deficit at high fluxes in Figure 8 might be related to saturation of the LAS (see Section 5). The surplus close to neutral conditions is also visible in Figure 7 of Meijninger et al. (2002b). A plausible explanation for this effect lies in the contrast in footprint scale and the heterogeneity in the LITFASS area. Net radiation and soil heat flux data are *in situ* measurements while the scintillometer data are path-integrated measurements (i.e., m^2 versus km^2 area scales). For example, a scintillometer can 'see' a number of different patches that have their stability transition at different times, while *in situ* measurements show a distinctive transition. This problem also arises when using *in-situ* measurements in the LAS–MWS method, in particular R_{TQ}. As mentioned before, in this study we used local r_{TQ} data (from a nearby EC station) for deriving C_T^2 and C_Q^2. During near-neutral conditions it regularly occurs that the EC system and the scintillometers have their stability transition at slightly different times. As a result C_T^2 and C_Q^2 (and the derived fluxes H and $L_v E$) are affected by an 'incorrect' sign of R_{TQ}, despite the fact that in most cases its value is close to zero. The bichrometic method of Ludi et al. (2005) should overcome this problem. Finally, the overestimation of the surface fluxes by the LAS–MWS system can be

related to the non-linearity between the structure parameters and the fluxes (see Section 5).

5. Discussion

As shown in Section 2.1 a scintillometer actually measures structure parameters (C_n^2) and not the flux. The relation between the structure parameters (C_T^2 and C_Q^2) and the surface fluxes of sensible heat and latent heat is non-linear. In the free convective limit they are related as follows (Kohsiek, 1982b)

$$H_{fc} \cong z\left(\frac{g}{T}\right)^{\frac{1}{2}} \left(C_T^2\right)^{\frac{3}{4}}, \tag{9}$$

$$L_v E_{fc} \cong z\left(\frac{g}{T}\right)^{\frac{1}{2}} \left(C_T^2\right)^{\frac{1}{4}} \left(C_Q^2\right)^{\frac{1}{2}}. \tag{10}$$

Over heterogeneous areas, such as the LITFASS area, this non-linearity leads to a systematic overestimation of the scintillometer fluxes (Lagouarde et al., 2002; Meijninger et al., 2002a,b). In Figure 10 this non-linearity effect above a moderate heterogeneous surface is schematically visualized. This example shows a LAS–MWS set-up (at a height of 40 m) installed

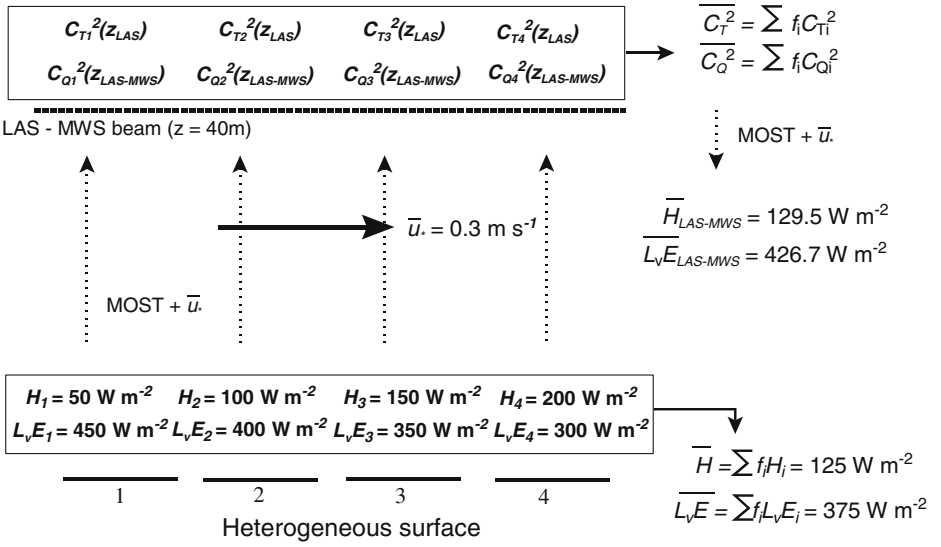

Figure 10. Schematic example showing the non-linearity between C_T^2 (C_Q^2) and $H(L_vE)$ and the resulting overestimation of the LAS–MWS fluxes by $5\,\mathrm{W\,m^{-2}}$ (4%) for $H(\Delta H = \overline{H_{\mathrm{LAS-MWS}}} - \overline{H})$ and $52\,\mathrm{W\,m^{-2}}$ (14%) for $L_vE(\Delta L_vE = \overline{L_vE_{\mathrm{LAS-MWS}}} - \overline{L_vE})$.

over an area consisting of four different patches with varying Bowen ratios (*Bo* varies from 0.11, 0.40, 0.43 to 0.67). It is assumed that the signatures of the four patches are still visible at the scintillometer height (i.e., no blending) and that there is no spatial variation in net radiation and soil heat flux. Once the fluxes of sensible heat are averaged (H_1 to H_4) one finds a mean flux of $125\,\mathrm{W\,m^{-2}}$. If one averages the structure parameters (C_{T1}^2 to C_{T4}^2, which have been derived from H_1 to H_4 using MOST and $\overline{u_*}$), the aggregated $\overline{C_T^2}$ will give a flux of $130\,\mathrm{W\,m^{-2}}$ (using MOST again and $\overline{u_*}$) instead of the expected $125\,\mathrm{W\,m^{-2}}$, i.e., the flux is $5\,\mathrm{W\,m^{-2}}$ higher. The same occurs with the latent heat flux, which is even further enhanced by the already 'incorrect' H (and related stability L_{Ob}). The overestimation mainly depends on the magnitude of the inhomogeneity (i.e., ΔH and $\Delta L_v E$) and the height of the scintillometers (the effect of contrast in surface roughness is much smaller (Lagouarde et al., 2002)). Interesting to note is that the overestimation of the sensible heat flux becomes smaller when the scintillometers are installed at a higher level, while the overestimation of the latent heat flux further increases. We must emphasize that this example is a worst-case scenario. In reality the signatures of the individual fields will have been (partly) blended by turbulent mixing once transported to higher levels (i.e. at scintillometer height). Note that we did not include the spatial weighting function of the LAS and MWS, i.e., all patches have been weighed equally (e.g., f_1 to $f_4 = 25\%$). According to Lagouarde et al. (2002) this will introduce an additional source of nonlinearity. Based on the *in situ* EC measurements (H_1 to H_x, $L_v E_1$ to $L_v E_x$ and $\overline{u_*}$) we have calculated the overestimation of H and $L_v E$ by the LAS – MWS combination. We found a systematic overestimation of 2% and 4% for H and $L_v E$, respectively.

Another effect that has been considered here is the reflection of electromagnetic waves via the ground (so called multipath propagation). Based on the set-up of the MWS (path length and height) the most serious reflection occurs at an angle of about 1°. According to the antenna pattern specifications of the receiver the sensitivity at that angle is reduced by more than 20 dB (i.e., a factor of 100) (Martin, 1999). Moreover, the ground is not a perfect reflector, which further reduces the chance of ground reflections. Note that low atmospheric inversions might also reflect electromagnetic waves. We expect the latter will play a role during nighttime conditions.

As mentioned in Section 2 we have used r_{TQ} data for estimating C_T^2 and C_Q^2. Lüdi et al. (2005) showed that the usage of r_{TQ} measurements instead of assuming a perfect correlation will lead to improved (reduced) C_Q^2 values. We found that the r_{TQ} measurements (which varied between -0.5 and 0.9) reduced C_Q^2 on average by 13%, implying that even larger latent heat fluxes were found when we assumed perfect correlation. Finally,

the measured r_{TQ} values, which are smaller than 1, imply that MOST is violated (Hill, 1997). However, the fact that r_{TQ} for most situations has a value of 0.7 or higher, indicates that the violation of MOST is small (Lüdi et al., 2005). This is also supported by the results presented here.

Kohsiek et al. (2006) investigated the performance of a XLAS (a LAS with an aperture diameter of 0.32 m), which was used also during LITFASS-2003. They discovered that the XLAS measurements suffered from saturation, but after correcting the XLAS measurements based on Hill and Clifford (1981), a satisfying agreement was found between the XLAS and the aggregated EC sensible heat fluxes. In addition they also mentioned that the saturation criterion given in Equation (2) is not strict enough, suggesting that once the saturation limit is reached saturation is already taking place, leading to underestimated fluxes ($\approx$ 20%). In the LAS–MWS set-up the LAS saturation criterion was reached regularly, indicating that the LAS is underestimating the sensible heat flux at high values. The findings of Kohsiek et al. (2006) might explain the energy gap in Figure 8 at high fluxes. This means that correcting the LAS for saturation will improve the energy balance closure, and thereby become more consistent with the findings of Meijninger et al. (2002b). However, on the other hand, the overestimation of the LAS compared to the aggregated EC fluxes (Figures 5 and 6) will become larger. As noted before, the MWS is not affected by saturation, as the measured C_n^2 values are much smaller than the saturation criterion (see Sections 2 and 3).

Finally, we must point out that other effects might play a role in the imbalance of both the LAS–MWS and EC observations (see e.g., Mahrt, 1998). For example, it is possible that part of the mean flux, which is related to the heterogeneity or topography, is not sensed by the measurement systems. Foken et al. (2006) performed a study on the energy balance closure problem on a selected EC dataset from the LITFASS-2003 experiment, and found that contributions to the turbulent fluxes in the longwave part of the spectrum have a significant influence on the imbalance. Their findings correspond with the work of Manabu et al. (2004), who used a large-eddy simulation model to show that the negative imbalance of EC measurements is attributed to local advection effects caused by low frequency turbulent organised structures.

6. Conclusions

In this LITFASS-2003 study we have investigated the performance of a combined Large Aperture and Millimetre Wave Scintillometer (LAS–MWS) for estimating area-representative surface fluxes of sensible and latent heat over a (moderate) heterogeneous landscape. We found that the sensible

heat fluxes from the LAS–MWS agree reasonably well with the aggregated EC fluxes. For the latent heat fluxes we found that the LAS–MWS fluxes were approximately 25% higher than the EC fluxes. This 25% difference is roughly equal to the difference in the surface energy balance closure of both systems. Our LAS–MWS results with a MWS at 94 GHz are similar to those of Meijninger et al. (2002b) who used a LAS–MWS combination with a MWS at 27 GHz. Considering the uncertainty of the Monin-Obukhov stability functions, the non-linearity between fluxes and structure parameters, saturation effects, and the still debatable energy gap of the EC measurements, the agreement between the LAS–MWS and EC measurements is encouraging. This study demonstrates that the LAS–MWS 'two-wavelength' method (plus r_{TQ} measurements, i.e., assuming non-ideal Tq correlation), as well as the single LAS, can be applied over moderate heterogeneous areas and can provide acceptable fluxes of both sensible and latent heat at scales of several kilometres.

Acknowledgements

We thank Aline van den Kroonenberg, Dion van den Bersselaar and Celso von Randow for their valuable assistance during the field experiment. We also acknowledge the constructive comments of the anonymous reviewers. This study was supported by the Dutch Science Foundation NWO (www.nwo.nl, project number 813.03.007).

References

Andreas, E. L.: 1988, 'Estimating C_n^2 over Snow and Sea Ice from Meteorological Data', *J. Opt. Soc. Amer.* **5**, 481–495.

Andreas, E. L.: 1989, 'Two-Wavelength Method of Measuring Path-Averaged Turbulent Surface Heat Fluxes', *J. Atmos. Ocean. Tech.* **6**, 280–292.

Andreas, E. L.: 1990, 'Three-Wavelength Method of Measuring Path-Averaged Turbulent Heat Fluxes', *J. Atmos. Ocean. Tech.* **7**, 801–813.

Andreas, E. L.: 1991, 'Using Scintillation at Two Wavelengths to Measure Path-Averaged Heat Fluxes in Free Convection', *Boundary-Layer Meteorol.* **54**, 167–182.

Bange, J., Herold, M., Spieβ, T., Beyrich, F., and Hennemuth, B.: 2006, 'Turbulent Fluxes from Helipod Flights above the Heterogeneous LITFASS Area', *Boundary-Layer Meteorol.*, this issue.

Beyrich, F., De Bruin, H. A. R., Meijninger, W. M. L., and Schipper, F.: 2002a, 'Experiences from One-Year Continuous Operation of a Large Aperture Scintillometer over a Heterogeneous Land Surface', *Boundary-Layer Meteorol.* **105**, 85–97.

Beyrich, F., Foken, T., and Herzog, H. J.: 2002b, 'The LITFASS-98 Experiment', *Theor. Appl. Climatol.* **73**(1–2), 1–2.

Beyrich, F. and Mengelkamp, H. T.: 2006, 'Evaporation over a Heterogeneous Land Surface: EVA_GRIPS and the LITFASS-2003 Experiment – An Overview', *Boundary-Layer Meteorol.*, this issue.

Beyrich, F., Leps, J-P., Mauder, M., Foken, T., Bange, J., Huneke, S., Lohse, H., Lüdi, A., Meijninger, W. M. L., Mironov, D., Weisensee, U., and Zittel, P.: 2006, 'Area-averaged Surface Fluxes over the LITFASS Region from Eddy-Covariance Measurements', *Boundary-Layer Meteorol.,* this issue.

Chehbouni, A., Watts, C., Lagouarde, J.-P., Kerr, Y. H., Rodriguez, J.-C., Bonnefond, J.-M., Santiago, F., Dedieu, G., Goodrich, D. C., and Unkrich, C.: 2000, 'Estimation of Heat and Momentum Fluxes over Complex Terrain Using a Large Aperture Scintillometer', *Agric. For. Meteorol.* **105**, 215–226.

Clifford, S. F.: 1971, 'Temporal-Frequency Spectra for a Spherical Wave Propagating through Atmospheric Turbulence', *J. Opt. Soc. Amer.* **61**, 1285–1292.

Clifford, S. F., Ochs, G. R., and Lawrence, R. S.: 1974, 'Saturation of Optical Scintillation by Strong Turbulence', *J. Opt. Soc. Amer.* **64**(2), 148–154.

De Bruin, H. A. R.: 1989, 'Physical Aspects of the Planetary Boundary Layer with Special reference to Regional Evapotranspiration', in *Proceedings of the Workshop on the Estimation of Areal Evapotranspiration*, Vancouver, BC, August 9–22, 1987, IAHS Publ. 177, pp. 117–132.

De Bruin, H. A. R., Kohsiek, W., and Van den Hurk, B. J. J. M.: 1993, 'A Verification of Some Methods to Determine the Fluxes of Momentum, Sensible Heat and Water Vapour using Standard Deviation and Structure Parameter of Scalar Meteorological Quantities', *Boundary-Layer Meteorol.* **63**, 231–257.

De Bruin, H. A. R., Van den Hurk, B. J. J. M., and Kohsiek, W.: 1995, 'The Scintillation Method Tested Over a Dry Vineyard Area', *Boundary-Layer Meteorol.* **76**, 25–40.

Foken, T., Wimmer, F., Mauder, M., Thomas, C., and Liebethal, C.: 2006, 'Some Aspects of the Energy Balance Closure Problem', *Boundary-Layer Meteorol.*, this issue.

Green, A. E., Green, S. R., Astill, M. S., and Caspari, H. W.: 2000, 'Estimating Latent Heat Flux from a Vineyard Valley Using Scintillometry', *J. Terres. Atmos. Ocean. Sci.* **11**(2), 525–542.

Green, A. E., Astill, M. S., McAneney, K. J., and Nieveen, J. P.: 2001, 'Path-Averaged Surface Fluxes Determined from Infrared and Microwave Scintillometers', *Agric. For. Meteorol.* **109**, 233–247.

Hartogensis, O. K., Watts, C. J., Rodriguez, J-C., and De Bruin, H. A. R.: 2003, 'Derivation of an Effective Height for Scintillometers: La Poza Experiment in Northwest-Mexico', *J. Hydro-Meteorol.* **4**(5), 915–928.

Hill, R. J., Clifford, S. F., and Lawrence, R. S.: 1980, 'Refractive Index and Absorption Fluctuations in the Infrared Caused by Temperature, Humidity and Pressure Fluctuations', *J. Opt. Soc. Amer.* **70**(10), 1192–1205.

Hill, R. J. and Clifford, S. F.: 1981, 'Theory of Saturation of Optical Scintillation by Strong Turbulence for Arbitrary Refractive-Index Spectra', *J. Opt. Soc. Amer.* **71**, 675–686.

Hill, R. J., Bohlander, R. A., Clifford, S. F., McMillan, R. W., Priestley, J. T., and Schoenfeld, W. P.: 1988, 'Turbulence-Induced Millimetre-Wave Scintillation Compared with Micro-Meteorological Measurements', *IEEE Trans. Geosci. Remote Sens.* **26**, 330–342.

Hill, R. J.: 1997, 'Algorithms for Obtaining Atmospheric Surface-Layer Fluxes from Scintillation Measurements', *J. Atmos. Ocean. Tech.* **14**, 456–467.

Horst, T. W. and Weil, J. C.: 1992, 'Footprint Estimation for Scalar Flux Measurements in the Atmospheric Surface Layer', *Boundary-Layer Meteorol.* **59**, 279–296.

Horst, T. W. and Weil, J. C.: 1994, 'How Far is Far Enough? The Fetch Requirements for Micrometeorological Measurements of Surface Fluxes', *J. Atmos. Ocean. Tech.* **11**, 1018–1025.

Kohsiek, W.: 1982a, *Optical and In Situ Measuring of Structure Parameters Relevant to Temperature and Humidity, and Their Application to the Measuring of Sensible and Latent Heat Flux*, NOAA Tech. Memor. ERL WPL-96, NOAA Environmental Research Laboratories, Boulder, CO, USA, 64 pp.

Kohsiek, W.: 1982b, 'Measuring C_T^2, C_q^2 and C_{Tq} in the Unstable Surface Layer, and Relations to the Vertical Fluxes of Heat and Moisture', *Boundary-Layer Meteorol.* **24**, 89–107.

Kohsiek, W. and Herben, M. H. A. J.: 1983, 'Evaporation Derived from Optical and Radio Wave Scintillation', *Appl. Optics.* **22**, 2566–2569.

Kohsiek, W., Meijninger, W. M. L., De Bruin, H. A. R., and Beyrich, F.: 2006, 'Saturation of the Large Aperture Scintillometer', *Boundary-Layer Meteorol.*, this issue.

Lagouarde, J-P., McAneney, K. J., and Green, A. E.: 1996, 'Scintillometer Measurements of Sensible Heat Flux over Heterogeneous Surfaces' in J. B. Stewart, E. T. Engman, R. A. Feddes and Y. Kerr (eds.), *Scaling Up in Hydrol. using Remote Sensing*, John Wiley, Chichester, U.K., pp. 147–160.

Lagouarde, J-P., Bonnefond, J-M., Kerr, Y. H., McAneney, K. J., and Irvine, M.: 2002, 'Integrated Sensible Heat Flux Measurements of a Two-Surface Composite Landscape using Scintillometry', *Boundary-Layer Meteorol.* **105**, 4–37.

Lüdi, A., Beyrich, F., and Mätzler, C.: 2005, 'Determination of the Turbulent Temperature-Humidity Correlation from Scintillometric Measurements', *Boundary-Layer Meteor.*, in press.

Mahrt, L.: 1998, 'Flux Sampling Errors for Aircraft and Towers', *J. Atmos. Oceanic Tech.* **15**, 416–429.

Manabu, K., Atsushi, I., Letzel, M. O., Raasch, S., and Watanabe, T.: 2004, 'LES Study of the Energy Imbalance Problem with Eddy Covariance Fluxes', *Boundary-Layer Meteorol.* **110**, 381–404.

Martin, L., 1999, 'Transmissionsmessungen in der Troposphäre bei 94 GHz', M.Sc. Thesis, University of Bern, Bern, Switzerland.

Mauder, M., Liebethal, C., Göckede, M., Leps, J-P., Beyrich, F., and Foken, T.: 2006, 'Processing and Quality Control of Flux Data during LITFASS-2003', *Boundary-Layer Meteorol.*, this issue.

Meijninger, W. M. L., Hartogensis, O. K., Kohsiek, W., Hoedjes, J. C. B., Zuurbier, R. M., and De Bruin, H. A. R.: 2002a, 'Determination of Area Averaged Sensible Heat Fluxes with a Large Aperture Scintillometer over a Heterogeneous Surface – Flevoland Field Experiment', *Boundary-Layer Meteorol.* **105**, 37–62.

Meijninger, W. M. L., Green, A. E., Hartogensis, O. K., Kohsiek, W., Hoedjes, J. C. B., Zuurbier, R. M., and De Bruin, H. A. R.: 2002b, 'Determination of Area Averaged Water Vapour Fluxes with Large Aperture and Radio Wave Scintillometers over a Heterogeneous Surface – Flevoland Field Experiment', *Boundary-Layer Meteorol.* **105**, 63–83.

Moene, A. F.: 2003, 'Effects of Water Vapour on the Structure Parameter of the Refractive Index for Near-Infrared Radiation', *Boundary-Layer Meteorol.* **107**, 635–653.

Nieveen, J. P., Green, A. E., and Kohsiek, W.: 1998, 'Using a Large-Aperture Scintillometer to Measure Absorption and Refractive Index Fluctuations', *Boundary-Layer Meteorol.* **87**, 101–116.

Ochs, G. R. and Wilson, J. J.: 1993, *A Second-Generation Large Aperture Scintillometer*, NOAA Tech. Memor. ERL ETL-232, NOAA Environmental Research Laboratories, Boulder, CO, USA, 24 pp.

Otto, W. D., Hill, R. J., Sarma, A. D., Wilson, J. J., Andreas, E. L., Gosz, J. R., and Moore, D. I.: 1996, *Results of The Millimeter-Wave Instrument Operated at Sevilleta, New Mexico*, NOAA Tech. Memor. ERL ETL-262, NOAA Environmental Research Laboratories, Boulder, CO, USA, 47 pp.

Panofsky, H. A. and Dutton, J. A.: 1984, *Atmospheric Turbulence, Models and Methods for Engineering Applications*, John Wiley & Sons, New York, 397 pp.

Sarma, A. D. and Hill, R. J.: 1996, *A Millimeter Wave Scintillometer for Flux Measurements*, NOAA Tech. Memor. ERL ETL-259, NOAA Environmental Research Laboratories, Boulder, CO, USA, 33 pp.

Shuttleworth, W. J.: 1988, 'MacroHydrology – The New Challenge for Process Hydrology', *J. Hydrol.* **100**, 31–56.

Troen, I. and Petersen, E. L.: 1989, *European Wind Atlas*, Risø National Laboratory, Røskilde, Denmark, 656 pp.

Wang, T. I., Ochs, G. R., and Clifford, S. F.: 1978, 'A Saturation-Resistant Optical Scintillometer to Measure C_n^2', *J. Opt. Soc. Amer.* **69**, 334–338.

Wesely, M. L.: 1976, 'The Combined Effect of Temperature and Humidity on the Refractive Index', *J. Appl. Meteorol.* **15**, 43–49.

Wyngaard, J. C., Izumi, Y., and Collins Jr., S. A.: 1971, 'Behaviour of the Refractive-Index-Structure Parameter Near the Ground', *J. Opt. Soc. Amer.* **61**, 1646–1650.